Preprints of the 19th World Congress
The International Federation of Automatic Control
Cape Town, South Africa. August 24-29, 2014

Kinetic Analysis and Optimization of Long Chain Branched Propylene Polymerization System

Anitha Mogilicharla, Saptarshi Majumdar, Kishalay Mitra*

**Indian Institute of Technology Hyderabad, Yeddumailaram 502205, Andhra Pradesh, INDIA*
(Tel:+91(0)40 2301 7055 e-mail: kishalay@iith.ac.in).

Abstract: A kinetic model has been proposed for a binary catalyst system with the available experimental data from the open literature, in which one catalyst produces polypropylene macromonomer, while the other catalyst attacks the macromonomers as side chains to the isotactic polypropylene backbone. After validating the model with the experimental data, it has been extended to find the optimal process conditions for the desired combination of conflicting objectives that leads to manufacturing of polymer with controlled branching suitable for varied kind of applications. A well-established multi-objective optimization technique, NSGA II, has been utilized for this purpose. Some of the Pareto optimal points are found to be better than the experimental data and show improvement in process performance.

1. INTRODUCTION

Due to the poor melt strength, linear polypropylene (PP) cannot be processed easily for applications like blow moulding, film forming etc. This aspect needs branching to be incorporated to the linear chains. Due to the lack of knowledge of the embedded chemistry to produce long chain branched polypropylene (LCBPP) by direct synthesis methods, other techniques such as reactive extrusion (Graebling, 2002) and electron beam irradiation (Auhl et al., 2004) became more popular in industrial practices. However, polymers produced by these methods exhibits broadened molecular weight distribution where it is difficult to control the extent of branching due to the complex distribution.

Due to the limited knowledge of the chemistry of LCBPP mechanism, various routes of LCBPP production have been studied. By the incorporation of insitu produced previously prepared vinyl terminated macromonomers, isotactic LCBPP can be produced (Weng et al., 2002). In this, long chain branching density depends on macromonomer insertion rate relative to the propylene monomer insertion rate. Shiono et al. (1999) used rac-Me_2Si (2-MeBenz[e]Ind)$_2ZrCl_2$ catalyst to copolymerize atactic polypropylene (aPP) macromonomer with propylene to produce LCBPP. LCBPP with isotactic backbones and atactic side chains have been produced by Ye and Zhu (2003) by the tandem catalysis. By this method, second catalyst copolymerizes the propylene monomer with vinyl terminated macromonomers that produced by the first catalyst to obtain LCBPP. By using the metallocene catalyst and T-reagent, Langston et al. (2008) produced LCBPP. In the presence of hydrogen, T-reagent acts as a chain transfer agent as well as comonomer. Apart from this, few kinetic models are developed for long chain branched polyolefin systems. Mehdiabadi et al. (2008) explained the series of two CSTRs performance with semi batch performance by considering the general olefin polymerization system, in which CSTRs showed the best performance in getting polymer with high long chain branching density.

However, Modeling of LCB PP with a proposed mechanism which can validate experimental findings is both a lacuna and an apparent necessity in the area of modeling and optimization of polymer reaction engineering system.

In the present effort, we have considered the example of LCB PP with binary catalyst system (Ye and Zhu, 2003) and presented a newly proposed kinetic mechanism which can validate experimental findings (Ye and Zhu, 2003). Dual catalyst systems have shown to be efficient to produce long chain branched polyethylene in a single reactor. Kinetic parameters are estimated by real coded genetic algorithm (Deb, 2001) by comparing with the experimental data from open literature. Furthermore, the above mentioned validated model is extended to find the optimal profiles of two catalysts, cocatalyst and second catalyst addition time that minimizes the total polymerization time while maximizing the iPP copolymer weight average molecular weight and grafting density (number of aPP side chains per 1000 iPP back bone monomer units) simultaneously. For this purpose, a well-established multi objective optimization technique non-dominated sorting genetic algorithm (NSGA II) has been utilized. To the best of our knowledge, this is the first effort for modeling the branched polypropylene system with experimental validation. Study for finding the optimal process conditions for such a process is extremely rare.

2. MODEL AND OPTIMIZATION

2.1 Model

All experimental runs (Ye and Zhu, 2003) were conducted at 1 atm. propylene pressure and 25°C in 200 ml of toluene solvent.The kinetic model for the above mentioned LCBPP with twin catalyst system is shown in Table 1. The model is validated with the experimental data (Ye and Zhu, 2003) from open literature, in which, C_1 and C_2 represents the concentrations of vacant active sites of first catalyst and second catalysts, respectively. P_n and $D_n^=$ represent the live and the unsaturated dead polymers (macromonomers) for

atactic polypropylene of chain length n, whereas, $Q_{n,i}$ and $R_{n,i}$ represent the live and the dead polymer chains of LCB PP respectively, having n numbers of chain length and i number of long chain branches (isotactic backbone and atactic side chains). The main chain transfer mechanism for the first catalyst system (1/MMAO) is β-hydride elimination (Small and Brookhart, 1999), which produces vinyl terminated macromonomers. Reinitiation occurs with the produced activated hydride catalyst complex (C_1^H). Reversible chain transfer mechanism has been considered for this to obtain polymer with narrow molecular distribution (Hustad et al., 2008), instead of Schulz-Flory distribution (polydispersity index = 2.0), more common for single site catalysts (Soares and Mckenna, 2012). For the second catalyst system (II/MMAO), chain transfer to cocatalyst (MMAO) has been considered as the chain transfer agent to avoid the formation of dendrimers (Zhu and Li, 1997). Second order deactivation has been considered for the second catalyst system which may be due to bimolecular deactivation (Soares and Mckenna, 2012). The present second catalyst has the capability of producing backbone (main chain) chains and at the same time, it connects the macromonomers as side chains to produce LCB PP.

From the kinetic mechanism (Table 1), the rate of formation of live and dead polymers can be derived and this leads to large number of equations. Method of moments has been utilized to reduce it to a lower order system (Table 2). Atactic polypropylene (aPP) live and dead polymer moments are represented from equation 2.1, while isotactic (iPP) copolymer live and dead polymer moments are represented in equation 2.2. Number average molecular weight (M_n), weight average molecular weight (M_w) and PDI are shown in equation 2.3 followed by grafting density (number of aPP side chains per 1000 iPP backbone monomer units) in equation 2.4. Here, M_W denotes the molecular weight of propylene.

Table 1: Kinetic mechanism for the bi catalyst system

First catalyst system

- Initiation
$$C_1 + M \xrightarrow{k_{i1}} P_1$$
- Propagation
$$P_n + M \xrightarrow{k_{p1}} P_{n+1}$$
- β - H elimination
$$P_n \xrightarrow{k_\beta} D_n^= + C_1^H$$
- Reversible chain transfer to metal
$$D_n^= + C_1^H \xrightarrow{k_{\beta r}} P_n$$
- Reinitiation
$$C_1^H + M \xrightarrow{k_{ri1}} P_1$$

Second catalyst system

- Catalyst activation
$$cat_2 + cocat \xrightarrow{k_{a2}} C_2$$
- Initiation
$$C_2 + M \xrightarrow{k_{i2}} Q_{1,0}$$
- Propagation
$$Q_{n,i} + M \xrightarrow{k_{p2}} Q_{n+1,i}$$
- long chain branching
$$Q_{n,i} + D_{m,0}^= \xrightarrow{\alpha k_{lcb}} Q_{n+m,i+1}$$
- Chain transfer to coctalyst
$$Q_{n,i} + cocat \xrightarrow{k_{al}} R_{n,i} + C_2^{Me}$$
- Reinitiation
$$C_2^{Me} + M \xrightarrow{k_{ral}} Q_{1,0}$$
- Bimolecular deactivation
$$2Q_{n,i} \xrightarrow{k_{d2}} 2R_{n,i} + 2C_d$$

Table 2: Moment rates of live and dead polymer chains for the binary catalyst system

$$\frac{d\lambda_0}{dt} = k_{i1}C_1M + k_{ri1}C_1^HM - k_\beta\lambda_0 + k_{\beta r}\mu_0^=C_1^H$$
$$\frac{d\lambda_1}{dt} = k_{i1}C_1M + +k_{ri1}C_1^HM + k_{p1}M\lambda_0 - k_\beta\lambda_1 + k_{\beta r}\mu_1^=C_1^H$$
$$\frac{d\lambda_2}{dt} = k_{i1}C_1M + +k_{ri1}C_1^HM + k_{p1}M(2\lambda_1 + \lambda_0) - k_\beta\lambda_2 + k_{\beta r}\mu_2^=C_1^H$$
$$\frac{d\mu_0^=}{dt} = k_\beta\lambda_0 - k_{\beta r}\mu_0^=C_1^H - \alpha k_{1cb}\mu_0^=\mu_0$$
$$\frac{d\mu_1^=}{dt} = k_\beta\lambda_1 - k_{\beta r}\mu_1^=C_1^H - \alpha k_{1cb}\mu_1^=\mu_0$$
$$\frac{d\mu_2^=}{dt} = k_\beta\lambda_2 - k_{\beta r}\mu_2^=C_1^H - \alpha k_{1cb}\mu_2^=\mu_0$$

$$\frac{d\mu_0}{dt} = k_{i2}C_2M + k_{ral}C_2^{Me}M - (k_{al}[cocat] + k_{d2}\mu_0)\mu_0$$
$$\frac{d\mu_1}{dt} = k_{i2}C_2M + k_{ral}C_2^{Me}M + (k_{p2}M + \alpha k_{1cb}\mu_1^=)\mu_0 - (k_{al}[cocat] + k_{d2}\mu_0)\mu_1$$
$$\frac{d\mu_2}{dt} = k_{i2}C_2M + k_{ral}C_2^{Me}M + k_{p2}M(2\mu_1 + \mu_0) - (k_{al}[cocat] + k_{d2}\mu_0)\mu_2 + \alpha k_{1cb}(2\mu_1\mu_1^= + \mu_0\mu_2^=)$$
$$\frac{d\nu_0}{dt} = (k_{d2}\mu_0 + k_{al}[cocat])\mu_0$$
$$\frac{d\nu_1}{dt} = (k_{d2}\mu_0 + k_{al}[cocat])\mu_1$$
$$\frac{d\nu_2}{dt} = (k_{d2}\mu_0 + k_{al}[cocat])\mu_2$$

$$\lambda_x = \sum_{n=1}^{\infty} n^x P_x \quad \mu_x^= = \sum_{n=1}^{\infty} n^x D_x^= \qquad (2.1)$$

$$\mu_x = \sum_{n=1}^{\infty} n^x Q_x \quad \nu_x = \sum_{n=1}^{\infty} n^x R_x \qquad (2.2)$$

$$M_n = \left(\frac{\nu_1}{\nu_0}\right)MW \quad M_w = \left(\frac{\nu_2}{\nu_1}\right)MW \quad PDI = \left(\frac{M_w}{M_n}\right) \qquad (2.3)$$

$$GD = 1000\left(\frac{\text{Long chain branching formation rate}}{\text{Propagation rate}}\right) \qquad (2.4)$$

In this binary catalyst system, first catalyst system (2-ArN=C(Me)]$_2C_5H_3N$}$FeCl_2$/MMAO (1))(Ye and Zhu, 2003) produces macromonomers, while the second catalyst system (rac-Me_2Si(2-MeBenz[e]Ind)$_2ZrCl_2$/MMAO (2)) (Ye and Zhu, 2003) copolymerizes aPP macromonomers with the propylene monomer to create long chain branches. Here, the grafting density depends on the time gap between the two catalyst additions (Ye and Zhu, 2003) and the ratio of two catalyst concentrations (Ye and Zhu, 2003). In other words, if both catalysts are added once, grafting density is zero. This may be due to the precipitation of isotactic polypropylene around the active sites of second catalyst, which inhibits the diffusion of macromonomer. If more time gap is allowed between the two catalyst additions, more amounts of

macromonomers will be grafted to the iPP back bone which is due to the accumulation of more amounts of macromonomers before the second catalyst addition (Ye and Zhu, 2003). Based on this explanation, one parameter α has been introduced apart from the kinetic constants and estimated by comparing with the experimental data to take care of this diffusional effect (i.e. all macromonomers will not be available to attack to the iPP back bone). Based on the experimental conditions, different α values are predicted depending on the grafting density. Based on these values, an empirical relation has been developed for α which is a function of time gap between the two catalyst additions, Fe/Zr ratio (i.e. first catalyst to second catalyst ratio) and copolymerization time. These parameters are estimated with the comparison of experimental and simulated values by minimizing the error (e) expression shown in equation 2.5. To cater this, model which is embedded with LIMEX DAE solver is integrated with the optimization routine, the real coded genetic algorithm (RCGA) (Deb, 2001).

$$e = \sum_{1}^{5}\left(\frac{M_{w,appsim} - M_{w,appexp}}{M_{w,appexp}}\right)^2 + \sum_{1}^{5}\left(\frac{PDI_{appsim} - PDI_{appexp}}{PDI_{appexp}}\right)^2 + \sum_{1}^{5}\left(\frac{M_{w,ippsim} - M_{w,ippexp}}{M_{w,ippexp}}\right)^2 + \sum_{1}^{5}\left(\frac{PDI_{ippsim} - PDI_{ippexp}}{PDI_{ippexp}}\right)^2 + \sum_{1}^{3}\left(\frac{GD_{sim} - GD_{exp}}{GD_{exp}}\right)^2 \quad (2.5)$$

2.2 OPTIMIZATION

Two catalyst additions (u_1 and u_2), cocatalyst (MMAO) (u_3), second catalyst addition time (u_4) and total polymerization (t_p) are considered as decision variables. These decision variables are decided by the optimization routine. Minimization of total polymerization time, maximization of M_w and maximization of GD are considered as objective functions as this combination leads to high quality controlled branched polymer. These objectives are conflicting in nature. In other words, to obtain more M_w and GD, more polymerization time is needed. But, when M_w and GD are to be maximized, the minimization of time is required. The above mentioned problem formulation with relevant constraints is shown in Table 3. All decision variables (Ye and Zhu, 2003) are kept within the lower and upper bounds (min and max) which are chosen based on the ±10% of the entire experimental range. Multi objective optimization (MOOP) has been performed to obtain the trade off solutions among the various conflicting objectives by the integrating the validated model with the optimization routine, real coded non-dominated sorting genetic algorithm (NSGA II) (Deb, 2001).

Table 3: Multi-objective optimization problem formulation

$$\begin{aligned}
&Maximize \quad M_w \\
&Maximize \quad GD \\
&Minimize \quad t_p \\
&500000 \le M_w \le 700000 \\
&4500 \le \frac{cocat}{cat_2} \le 8000 \\
&M_{w,app} \ge 2500 \\
&PDI_{app} \le 1.45 \\
&GD \ge 7
\end{aligned}$$

The values of decision variables are

$$\begin{aligned}
&u_1^{min} = 14e^{-6} mol/lit; u_1^{max} = 82.5e^{-6} mol/lit \\
&u_2^{min} = 9e^{-6} mol/lit; u_2^{max} = 16.5e^{-6} mol/lit \\
&u_3^{min} = 0.045 mol/lit; u_3^{max} = 0.0825 mol/lit \\
&u_4^{min} = 0.2t_p; u_4^{max} = 0.8t_p \\
&t_p^{min} = 70\,\text{min}; t_p^{max} = 180\,\text{min}
\end{aligned}$$

3. RESULTS AND DISCUSSION

The kinetic mechanism proposed in the present paper is based on the following assumptions: (i) Two catalyst systems act as single center catalysts; (ii) Deactivation of second catalyst results from bimolecular deactivation (Soares and Mckenna, 2012). Comparison of model predicted and experimental M_w, polydispersity index (PDI) of aPP macromonomers is shown in Figure 1. Second catalyst system generates backbone chains and connects the side chains at the same time to obtain the comb branched polymers. Experimental and model predictions of iPP copolymer (LCBPP) are depicted in Figure 2. Polymer molecular properties of aPP and iPP copolymer are matched well with the experimental findings (Ye and Zhu, 2003). Grafting density (number of aPP side chains per 1000 iPP backbone monomer units) for different experimental runs is shown in Table 4. Comparisons of experimental and simulated values for the first three runs are matching quite well. Last two runs are predicted from model and these values are compared with the melting points (Ye and Zhu, 2003) of the iPP copolymer as the corresponding experimental values are not available. As the grafting density increases, iPP copolymer melting point decreases (Ye and Zhu, 2003). High melting point of 4th experimental run compared to 3rd experimental run indicates low grafting density.

Calculating the molecular weight distribution is important due to its direct relation with the polymer product quality. Figure 3 depicts the molecular weight long chain branching distributions for the second experimental run. This is calculated by the fractionation of total polymer into several classes based on the same long chain branching content (Yiannoulakis et al., 2000). In this method, total polymer population is divided into various classes based on the

number long chain branches (0, 1, 2 etc.). Overall molecular weight distribution is the weighed sum of all class distributions.

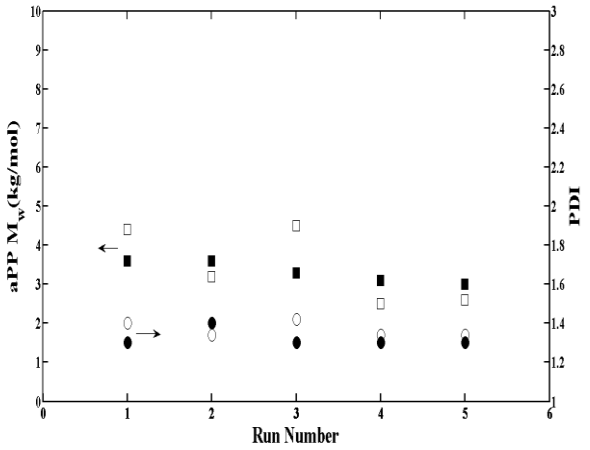

Fig. 1: Experimental M_w (filled square), predicted M_w (empty square) and experimental PDI (filled circle), predicted (empty circle) of aPP macromonomers.

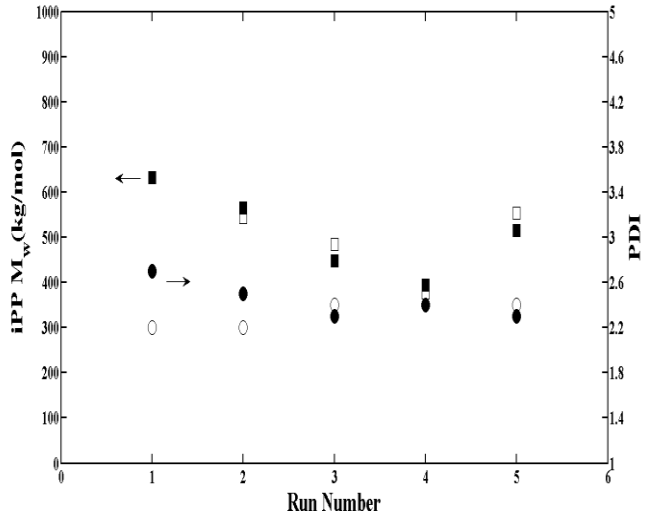

Figure 2: Experimental M_w (filled square), predicted M_w (empty square) and experimental PDI (filled circle), predicted (empty circle) of iPP copolymer (LCBPP).

Table 4: Comparison of experimental grafting density findings with the model predictions

Run No.	Zr:Fe:Al	Zr (μM)	Second catalyst addition time (min)
1	2:15:15000	10	90
2	2:15:15000	10	30
3	3:15:15000	15	120
4	3:15:15000	15	30
5	3:5:15000	10	30

Grafting Density		Melting Point
Experimental (Ye and Zhu, 2003)	Model	
8.4	8.2	144.4
1.7	1.7	148.6
8.6	7.5	145.6
	0.31	149.7
	0.008	153.5

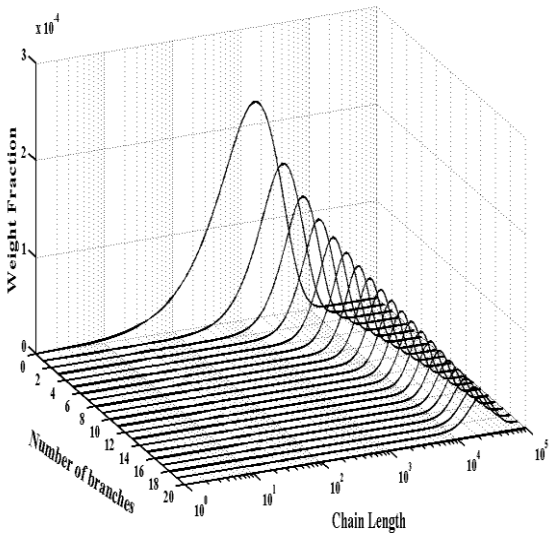

Fig. 3: Molecular weight distributions

After validating the model with the experimental data from open literature, it has been extended to investigate the process performance by multi objective optimization to attain desired combination of various conflicting objectives. Figure 4 represents the multi-objective trade off solutions for the above mentioned conflicting objectives. All decision variables are forced to lie within ±10% of the total experimental range to avoid the model extrapolation errors These Pareto optimal solutions are projected into the individual 2-d planes for better understanding of the situation. Experimental points of run 1 and run 3 (which are having grafting density greater than 8) are represented in the same plot as filled circles. Numbers of Pareto optimal solutions are found better than the data from the open literature (experimental).

Corresponding to the above Pareto optimal solutions (Figure 4), values of ratio of the two catalysts (catalyst 1/catalyst 2, i.e. Fe/Zr), grafting density and second catalyst addition time are shown in Figure 5 with copolymerization time represented in shades. From this Figure, it is evident that with lower catalyst ratio, the optimization routine has chosen more time gap between the two catalyst additions (i.e. second catalyst addition time) to achieve more GD in less

copolymerization time. However, lesser value of iPP M_w is obtained in less copolymerization time (Figure 6). In these solutions, higher M_w points appear for low cocatalyst concentration, which is due to low chain transfer to cocatalyst.

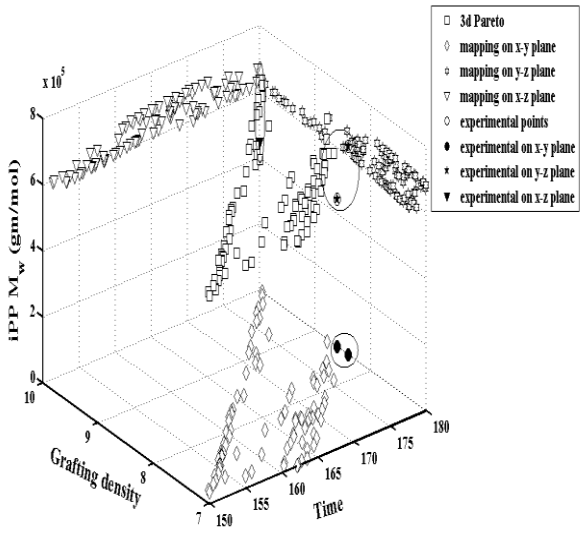

Fig. 4: Pareto optimal solutions (x: Time (min.), y: Grafting density, z: iPP M_w).

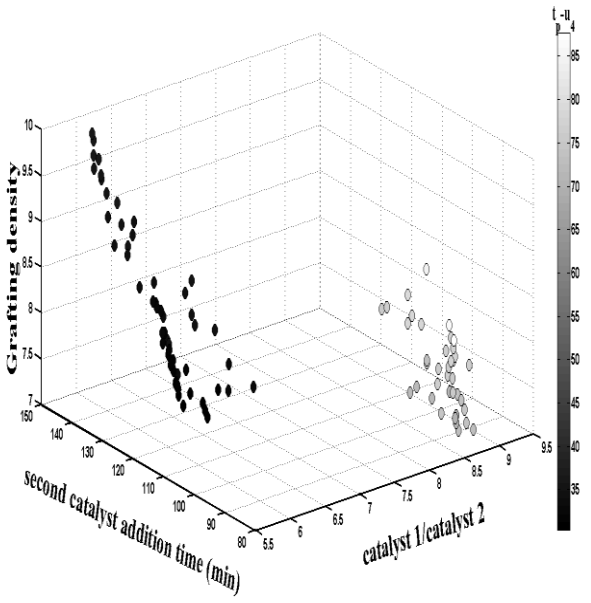

Fig. 5: Grafting density variation with the ratio of the two catalysts, second catalyst addition time (t_p-u_4: copolymerization time).

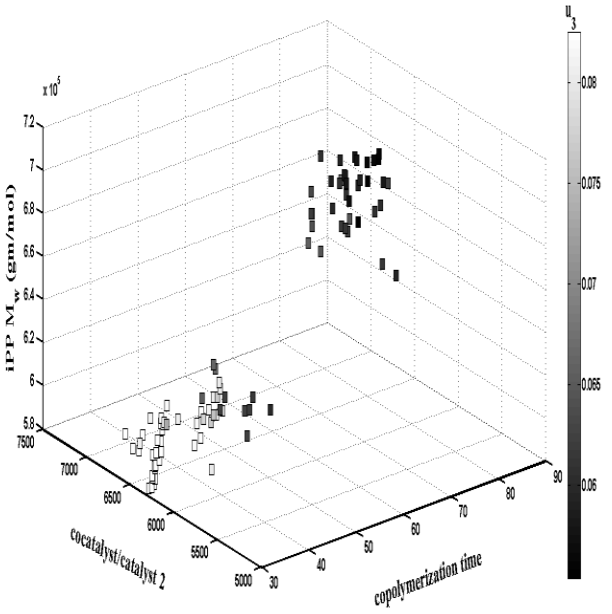

Fig. 6: Effect of copolymerization time, cocatalyst/catalyst 2 ratio on iPP molecular weight (u_3: cocatalyst concentration).

At the end of multi-objective optimization exercise, multiple numbers of trade-off solutions are obtained as opposed to a single solution in case of single objective optimization. However, finally, one has to choose only one solution as the solution of choice and this selection needs decision maker's knowledge about how to prioritize among various objectives.

4. CONCLUSIONS

Moment based modeling has been applied to an optimal control problem of LCBPP system to produce the tractable set of equations from an originally high dimensional problem. Multi-objective optimization has been formulated for various conflicting process objectives with relevant constraints for an experimentally validated model. Maximization of iPP weight average molecular weight and grafting density has been attained along with minimization of total polymerization time without violating the process constraints. Real coded NSGS II is used to get the optimal process conditions. Optimization routine provided wide variety of solutions in the entire terrain of the search sapce. First catalyst concentration, second catalyst concentration, cocatalyst concentration and time gap between the two catalyst additions are used as decision variables. One of the objective functions, grafting density, strongly depends on the time gap between the two catalyst additions, ratio of the two catalysts and copolymerization time. Other objective function iPP M_w depends on cocatalyst which is due to chain transfer to cocatalyst and Al/Zr ratio (bimolecular deactivation).

REFERENCES

Auhl, D., Stange, J., Munstedt, H., Krause, B., Voigt, D., Lederer,A., Lappan, U., Lunkwitz, K. (2004). Long-Chain Branched Polypropylenes by Electron Beam Irradiation and Their Rheological Properties. *Macromolecules*, **37 (25)**, 9465-9472.

Deb, K. (2001). *Multi-objective optimization using evolutionary algorithms*. Wiley, Chichester, UK.

Graebling, D. (2002). Synthesis of branched polypropylene by a reactive extrusion process. *Macromolecules*, **35 (12)**, 4602-4610.

Hustad, P.D., Kuhlman, R.L., Carnahan, E.M., Wenzel, T.T., Arriola, D.J. (2008). An exploration of the effects of reversibility in chain transfer to metal in olefin polymerization. *Macromolecules*, **41 (12)**, 4081-4089.

Langston, J.A., Colby, R.H., Mike Chung, T.C., Fumihiko Shimizu, Suzuki, T., Aoki, M. (2008). Synthesis and characterization of long chain branched isotactic polypropylene via metallocene catalyst and T-reagent. *Macromolecules*, **40 (8)**, 2712-2720.

Majumdar, S., Mitra, K., Raha, S. (2005) *Polymer*. **46**, 11858–11869.

Mitra, K., Majumdar, S., Raha, S. (2004). *Ind. Eng. Chem. Res.*, **43**, 6055-6063.

Mehdiabadi, S., Soares, J.B.P., Dekmezian,A.H., (2008). Production of Long-Chain Branched Polyolefins with Two Single-Site Catalysts: Comparing CSTR and Semi-Batch Performance. *Macromol. React. Eng.* **2**, 529-550.

Raha, S., Majumdar, S., Mitra, K. (2004). *Macromol. Theory Simul.* **13**, 152 – 161.

Shiono, T., Azad, S. M., Ikeda, T., (1999). Copolymerization of Atactic Polypropene Macromonomer with Propene by an Isospecific Metallocene Catalyst. *Macromolecules*, **32(18)**, 5723-5727.

Small, B. L., Brookhart, M. (1999). Polymerization of Propylene by a New Generation of Iron Catalysts: Mechanisms of Chain Initiation, Propagation, and Termination. *Macromolecules*. **32 (7)**, 2120-2130.

Soares, J.B.P., Mckenna, T.F.L. (2012). *Polyolefin Reaction Engineering*. Wiley.

Weng, W., Hu, W., Dekmerzian, A. H., Ruff, C. J. (2002). Long Chain Branched Isotactic Polypropylene. *Macromolecules*, **35 (10)**, 3838-3843.

Ye, Z., Zhu, S. J. (2003). Synthesis of branched polypropylene with isotactic backbone and atactic side chains by binary iron and zirconium single-site catalysts. *Polym. Sci., Part A: Polym. Chem.*, **41**, 1152-59.

Yiannoulakis, H., Yiagopoulos,A., Pladis, P., Kiparissides,C. (2000). Comprehensive dynamic model for the calculation of the molecular weight and long chain branching distributions in metallocene-catalyzed ethylene polymerization reactors. *Macromolecules*. **33**, 2757-66.

Zhu, S., Li, D. (1997). Molecular weight distribution of metallocene polymerization with long chain branching using a binary catalyst system. *Macromol. Theory Simul.* **6**, 793-803.